Open access • Journal Article • DOI:10.1038/S41565-018-0244-6

An integrated self-healable electronic skin system fabricated via dynamic reconstruction of a nanostructured conducting network. — Source link

Dong Hee Son, Jiheong Kang, Orestis Vardoulis, Yeongin Kim ...+17 more authors

Institutions: Stanford University, Kyung Hee University, Asahi Kasei, Samsung

Published on: 20 Aug 2018 - Nature Nanotechnology (Nature Publishing Group)

Topics: Electronic skin

An integrated self-healable electronic skin system fabricated via dynamic reconstruction of nanostructured conducting network

Donghee Son[1,2†], Jiheong Kang[1†], Orestis Vardoulis[1†], Yeongin Kim[3], Naoji Matsuhisa[1], Jin Young Oh[1], John WF To[1], Jaewan Mun[1], Toru Katsumata[1,6], Yuxin Liu[1], Allister F. McGuire[4], Marta Krason[1], Francisco Molina Lopez[1], Jooyeun Ham[5], Ulrike Kraft[3], Yeongjun Lee[1], Youngjun Yun[7], Jeffrey B.-H. Tok[1], Zhenan Bao[1]*

[1] *Department of Chemical Engineering, Stanford University, Stanford, CA 94305-5025, USA*

[2] *Biomedical Research Institute, Korea Institute of Science and Technology, 5, Hwarang-ro 14-gil, Seongbuk-gu, Seoul, 02791, South Korea*

[3] *Department of Electrical Engineering, Stanford University, Stanford, CA 94305-5025, USA*

[4] *Department of Chemistry, Stanford University, Stanford, CA 94305-5025, USA*

[5] *Department of Mechanical Engineering, Stanford University, Stanford, CA 94305-5025, USA*

[6] *Corporate Research and Development, Performance Materials Technology Center, Asahi Kasei Corporation, 2-1 Samejima, Fuji, Shizuoka 416-8501, Japan*

[7] *Samsung Advanced Institute of Technology Yeongtong-gu, Suwon-si, Gyeonggi-do 443-803, South Korea*

[†]*These authors contributed equally to this work*

*To whom correspondence should be addressed. *E-mail: zbao@stanford.edu*

Abstract: Electronic skin devices capable of monitoring physiological signals and displaying feedback information through closed-loop communication between user and electronics are being considered for next-generation wearables and Internet-of-Things. Such devices need to be ultrathin to achieve seamless and conformal contact with our human body, to accommodate strains from repeated movement and be comfortable to wear. Recently, self-healing chemistry has driven important advances in deformable and reconfigurable electronics, particularly with self-healable electrodes as the key enabler. Unlike polymer substrates with self-healable dynamic nature, the disrupted conducting network is unable to recover its stretchability after damage. Herein, we report the observation of self-reconstruction of conducting nanostructures when in contact with a dynamically crosslinked polymer network. This finding, combined with the self-bonding property of self-healing polymer, allowed subsequent heterogeneous multi-component device integration of interconnects, sensors and light emitting devices into a single multi-functional system. This first autonomous self-healable and stretchable multi-component electronic skin paves the way for future robust electronics.

Skin-inspired electronics have been applied to a variety of soft and deformable electronics for applications, such as wearable electronics[1-4], prosthetic artificial skin[5,6] and implantable medical devices[7] based on high-performance materials[8-17]. Self-healable materials that are developed to mimic the restorative nature of human skin have the potential to make thin and soft constructs of stretchable electronic devices extremely robust after incidental mechanical damages to prevent permanent breakdowns. Despite significant progresses in the development of self-healable materials[18-29], none has yet realised autonomous mechanical and electrical self-healing stretchable electrode and its integration into a multifunctional electronic system. This is primarily due to the challenges in device fabrication and lack of massive integration of individual self-healable electronic modules into a system.

Previously, Dickey et al. demonstrated the advantages of self-healing materials through a reconfigurable liquid-metal electrodes printed on a self-healing polymer[30]. Our group reported on stretchable self-healable electronic skin fabricated with liquid metal supported by a tough, stretchable and self-healable polymer[31]. However, even though liquid metal works well as interconnecting electrodes, it is not suitable as electrodes for active electronic components such as displays and physiological sensors. On the other hand, one-dimensional (1D) metal nanowires and carbon nanotubes have been used for self-healable electrodes[24,25]. However, they have not been shown stretchable after healing due to the inability for such nanostructure to recover its original connectivity[23].

In the field of supramolecular chemistry, it is well-established that self-assembled structures in solution can dynamically 'reconstruct' to a thermodynamic state[32]. In addition, the dynamic self-healing process is highly affected by the use of solvent vapor and temperature[32]. However, this phenomenon has yet been associated to macroscopic changes. Our results presented here

suggest that when a nanowire conductive network is surrounded by a self-healing polymer matrix, the broken conductive network can follow the dynamic reconstruction of the self-healing polymer and autonomously heal to recover not only the high conduction but also its mechanical properties. Moreover, they can be used as electrodes in active electronic components for sensors and displays. This enables the fabrication of various stretchable and self-healing electronic components. Taking advantage of the self-bonding property of the self-healing polymer and its high toughness, we report here the realisation of the first fully self-healable and stretchable multifunctional electronic skin system with a strain monitor, an electrocardiogram (ECG) sensor along with a light emitting capacitor (LEC) display array.

Dynamic reconstruction of nanostructured conductive network

We previously reported the design of PDMS-$MPU_{0.4}$-$IU_{0.6}$, which forms a crosslinked network with strong (4,4'–methylenebis(phenyl urea) unit, MPU) and weak (isophorone bisurea unit, IU) dynamic bonding units incorporated into the poly(dimethylsiloxane) backbone[31]. PDMS-$MPU_{0.4}$-$IU_{0.6}$ exhibits a high stretchability up to 1600% strain and a record-high fracture toughness of (~12,000 J/m^2) among any reported self-healing polymers (see Supplementary Section 1.1). We utilise this polymer due to its outstanding fracture toughness. However, the outline presented here should be applicable to other autonomous self-healing polymers.

After peeling off the film from the substrate, the conductive CNT network is primarily situated on the top surface of the film. We observed that the resistance of the CNT-network increased 10-times after the above embedding process, most likely due to some inter-penetration of the insulating polymer in between the CNTs. The electrical resistance of

the electrode can be improved by doping with Au salt (Supplementary Fig. 1a)[33]. To confirm if a stable conducting film is produced, we performed a simple 'scotch-tape test' while monitoring its resistance; in which its resistance values were observed to be reliable and stable (Supplementary Fig. 1). Next, we investigated the mechanical property of the CNT-network in polymer matrix while stretching up to 50% strain (Supplementary Fig. 5a, red). The resistance is observed to initially increase with strain, but subsequently showed less increase if strained up to a similar level. The change in resistance versus strain of our CNT electrode showed a similar behavior to those reported previously for stretchable CNT films on PDMS substrates[34].

To investigate the autonomous self-healing ability of our electrodes, we performed *in-situ* monitoring of its resistance against mechanical damages. First, we inflicted a surface-level cut on the electrode using a razor blade equipped with a force gauge to provide quantitative measure of the damage applied (Supplementary Fig. 2, see Supplementary Section 1.2). We subsequently inflicted various forces and consecutive damages (from 0.5 N to 4 N forces; 20 times of 2N force) at prescribed time intervals on the CNT-electrode (Fig. 2a and Supplementary Figs. 2b, 2d, and 2e). Interestingly, we observed autonomous self-healing of electrical conductivity for both cases after the cut and initial complete loss of conduction without using any force to push the two cut pieces into contact. However, when a more severe damage was introduced to the electrode, e.g. cutting with 4N force, we observed that the self-healing efficiency, as measured by electrical resistance, was lowered. We reasoned that damage caused by a higher force, i.e. 4N, induced a lower probability for intimate physical contact between the damaged surfaces, which prevents the full electrical recovery (Supplementary Figs. 3a and 3b). Additionally, we observed a continuous decrease in resistance over time without applying any external force, indicating that the conductive pathway was gradually being self-recovered, i.e. rearranged (Supplementary Fig. 2b). Its

electrical resistance was observed to recover from ∞ to 9 kΩ after a day.

To further confirm whether the damaged conductive network autonomously recovered its stretchability, we again made a surface cut on the CNT electrode with 2 N force and stretched it up to 200% strain after 12-hr at room temperature (Fig. 2d). The fact that a line-shaped damage on the CNT-electrode was blurred and stable even at the 200% strain after 12 h clearly supported recovered mechanical properties of the CNT nano-network. We further traced its self-healing process of conductive network with controlled self-healing time (Fig. 2c). We found that the resistance-strain behavior was improved by increasing healing time and finally became comparable to that of pristine sample, suggesting convergence time of about12 h for self-recovery of conductive pathway and its mechanical properties (Fig. 2c and 2d). After 2 days at room temperature, we observed that even the resulting scar on the healed electrode in the CNT network is almost indiscernible after healing (Supplementary Fig. 3c). In addition to this, when a complete cut was made on the CNT-electrode and brought together as an extreme self-healing case (Supplementary Figs. 4 and 5), after 24-hr at room temperature, our collected data (Supplementary Fig. 5e) showed that the self-healed conducting film had only a slightly increased (~17%) resistance, while the resistance-strain behavior was also almost identical to that of the pristine sample. This observation again suggested that the CNTs at the cut regions had to be truly intermixed and reconstructed in order to achieve such results.

To demonstrate the general applicability of the conductive network reconstruction enabled by our self-healing polymer matrix, we extended our investigation to AgNWs, which are also commonly utilised in stretchable conductors owing to its high conductivity[10]. We made a complete cut on electrodes and again reconnect them to investigate the reorganisation phenomenon of both CNT and silver nanowire (AgNW) nano-networks. We observed that the

129 resistance of the CNT (red) and AgNW (blue) electrodes decreased as soon as both bisected
130 interfaces make contact with each other and proceeds to further gradually decrease over time
131 (autonomous reconstruction of conductive network) (Fig. 2e). Therefore, this again suggests
132 that the dynamic reconstruction of CNT and AgNW nanostructured networks was enabled by
133 the dynamic movement of the polymer, which was subsequently reflected by its electrical
134 performance recovery, even when stretched.

135 The dynamic nature of the polymer network was investigated from its rheology
136 characterisation[31]. Previous studies suggested that faster polymer dynamics occurred on surface,
137 rather than bulk[35]. Since our CNT and AgNW conductive networks were mostly concentrated
138 on the polymer surfaces, its 'reconstruction' process may be further enhanced by the 'surface
139 effect'. In addition, Au doping can further improve the electrical properties of the electrode
140 (Supplementary Fig. 4b). We note that this autonomous reconstruction of a conducting network
141 has not been reported before. Since the cutting creates a complete break in the conducting
142 network, it would not become stretchable again unless the network rearranges if the two cut
143 pieces are simply placed in contact to each other. Our observation that the conducting network
144 recover its inherent ability to conduct under strain similar to the pristine un-cut network
145 suggests that the conducting network can be reconstructed to recover both the percolation
146 pathways for electrical conduction and the required morphology for high mechanical strength.
147 Notably, the SEM images of pristine and self-healed CNT (top)/AgNW (bottom)
148 nano-networks validated the reconstruction of nanostructured conductive networks after 12
149 hours at room temperature (Fig. 2f). To explain this observation, we reasoned that both the low
150 glass transition temperature of the polymer matrix and the dynamic crosslinking have
151 collectively provided the ability to transport the CNTs along with the polymer molecules to the
152 induced cracks/joints during the self-healing process. The stretchability of the self-healed

electrode can be readily confirmed by connecting our self-healed electrodes to a commercial light emitting diode (LED) (Supplementary Fig. 5). In specific, we observed that the LED remains "ON" while the self-healed CNT-electrode was being stretched up to 50% strain. Next, to investigate its robustness and toughness, we introduced a notch on the electrode (Supplementary Fig. 6e). Remarkably, even when stretched to a 100% strain, our electrode was still able to maintain good electrical conduction, which we attribute to its high fracture energy of polymer matrix. Such a performance is previously not observed for stretchable and self-healable solid-state conductors.

To further understand the autonomous self-healing of our conductive network, we next investigated the correlation between the self-healing process of our polymer matrix to the conductive network (Fig. 1b). First, we categorised the self-healing process of our electrode in two stages: (i) spontaneous physical contact after removal of razor blade, and (ii) reorganisation of CNT network during restructuring of the polymer matrix (Fig. 1c). We monitored the resistance change of electrodes prior and after damage, using several types of polymer matrixes, e.g. covalent crosslinked PDMS (Sylgard 184), thermoplastic SEBS and PDMS-IU. Surface cutting induced by a 2 N force was made into SEBS (elastic modulus 3.5 MPa), PDMS-$MPU_{0.4}$-$IU_{0.6}$ (0.7 MPa), PDMS (Sylgard 184, 0.7 MPa), respectively[31]. Compared to resistance changes of PDMS- or SEBS-supported CNT electrodes, the PDMS-$MPU_{0.4}$-$IU_{0.6}$ gave superior self-healability in terms of the final recovered resistance even though PDMS had similar or lower elastic modulus (Fig. 2g and Supplementary Fig. 6). Since SEBS and PDMS (Sylgard 184) polymer matrixes do not exhibit self-healability, their damaged electrodes lost their electrical properties again upon stretching and bisected again into two pieces (Fig. 2h and Supplementary Fig. 6d).

Stretchable conducting interconnects and sensors with autonomous self-healability

Owing to the high conductivity of the AgNW network, self-healable AgNW electrodes can be used as an efficient interconnect to interface with high-performance wearable electronic components. The AgNW/PDMS-$MPU_{0.4}$-$IU_{0.6}$ electrodes with different AgNW thicknesses (left, 114 nm (65.9 Ω at length of ~1.5 mm and width of 7 mm); center, 317 nm (46.3 Ω); right, 702 nm (34.0 Ω)) all showed good initial stretchability up to 50% strain without severe hysteresis (Figs. 3a and Supplementary Fig. 7a). The percolated network structure recovered after repeated damages (Fig. 3b). We observed that as AgNW thickness increased, damage recovery was correspondingly faster (Fig. 3b), most likely due to the increased physical contacts between AgNWs located along the bisected electrode edges. If there are slightly mismatched edges, slight increase in resistance was observed (Supplementary Fig. 7b). Last, even after making a complete cut on the AgNW/PDMS-$MPU_{0.4}$-$IU_{0.6}$ film and subsequently bringing it together, the electrode was autonomously healed at r.t. both electrically and mechanically again suggesting the reorganisation of the conducting nanostructures after cutting (Supplementary Fig. 8).

For wearable applications, self-healing performance should be maintained even in contact with sweat (Supplementary Fig. 9). Interestingly, the reconnected electrode can be stretched up to 50% strain, without significant electrical degradation, even after a day under artificial sweat (Fig. 3c). Furthermore, mechanical and electrical stability of the self-healable AgNW electrodes is reliable while touching and scratching (Supplementary Fig. 10). With this encouraging observation, we next incorporated the self-healable interconnects into a flexible circuit design with inorganic light emitting diodes (LEDs) as fabricated on a polyimide printed circuit board (Figs. 3d and Supplementary Figs. 11 and 12, see Supplementary Section 1.3).

The LED was operated using a digital communication protocol (Supplementary Fig. 12, see Supplementary Section 1.4 and Movie 1). We first made both partial and complete cuts on the self-healable interconnects and, subsequently, checked on the functionalities of each LED. After 24 h, we observed that the power source was electrically reconnected through the self-healable interconnects, even under an overall strain of ~34%.

Next, we employed our fabricated self-healing electrodes as active components in devices. In specific, a wearable self-healable ECG sensor composed of three electrodes was fabricated (Fig. 3e). The sensor was conformably attached on the human arm (Supplementary Fig. 13, see Supplementary Section 1.5). Damage recovery of the self-healable electrode was visualised via the recovery of real-time cardiac signal recordings (blue-coloured box in Fig. 3f; see Supplementary Movie 2). We observed that the signal was able to return to its normal baseline within seconds after damage was incurred. We note that EMG measurement is also possible using these electrodes (Supplementary Fig. 14; see Supplementary Section 1.5 and Movie 3). In addition, we developed a capacitive strain sensor comprised of PDMS-$MPU_{0.4}$-$IU_{0.6}$ dielectric (thickness of ~500 μm) sandwiched between the top and bottom self-healing electrodes (Supplementary Fig. 15). We observed that even after inflicting damages on the strain sensor, (inset in Fig. 3g), it nonetheless maintained reliable strain sensing performances within the strain range of human epidermis (~25% strain)[1], due to material homogeneity and a robust interface between the self-healable electrode and dielectric through H-bonding (Figs. 3g and 3h). Next, we introduced a notch into the strain sensor to examine any resulting crack propagation upon stretching (Fig. 3i). Remarkably, it was stretched up to 50% strain without further crack propagation.

Highly stretchable electroluminescent skin with autonomous self-healability

With our developed stretchable self-healing dielectric and electrodes, realisation of a both stretchable and self-healable display may now be possible. Previously, Shepherd and Suo reported a highly stretchable electroluminescent skin using an ionic hydrogel matrix, but it was not self-healable[36,37]. Thus, we proceed to prepare a composite with Cu-doped ZnS microparticles embedded in the PDMS-$MPU_{0.4}$-$IU_{0.6}$ polymer matrix as an emission layer (Supplementary Fig. 16, see Supplementary Section 1.6 and Methods). The active layer is then sandwiched between CNT- or AgNW self-healable electrodes. The capacitive behavior of the LEC structure was indistinguishable for pristine, self-healed and sample with a notch as a function of strain (Figs. 4a, and 4b, see Supplementary Section 1.7)[35]. Since PDMS-$MPU_{0.4}$-$IU_{0.6}$ can bond readily through H-bonding, such an assembly can be prepared through self-bonding between layers, which greatly simplified the fabrication process. The CNT-based LEC device can be stretched up to 250% strain, which is comparable to that of the hydrogel-based devices (Fig. 4c and Supplementary Figs. 17, 18 and 19)[36,37].

The autonomously self-healed LEC devices, based on either CNTs or AgNW electrodes, can be recovered completely to emit a blue-green light. Also, they did not suffer any significant degradation in the emitted light intensity at even ~50% strain after healed from a complete cut (Figs. 4d, 4e, and 4f and Supplementary Fig. 20). As a control test, we confirmed the self-healability and stretchability of the active emission layer without conducting layers (Supplementary Fig. 21). However, we also note that the recovery yield depends on the area of exposed surfaces in between the bisected edges. In this case, if the cross-sectional area of the conducting materials was increased, the yield was correspondingly improved[24]. Besides a complete cut test, we also made an incomplete cut on the LEC device, leaving behind a small connected part (at least ~50 μm thickness) on the bottom side of the self-healing substrate (Supplementary Figs. 22 and 23). In this case, it allowed proper contact alignment possible,

thereby maintaining a reliable photonic performance under tensile strain. With both self-healing functionality and the simple bonding assembly technology, our fabricated self-healable LEC exhibits reliable waterproof operation without electrical breakdown, even when stretched to >100% strain (Figs. 4g, 4h, and 4i).

Integrated electronic skin with autonomous self-healability

With the above materials and simple bonding fabrication process enabled by dynamic bonds and high fracture toughness through our developed self-healing polymer, we proceed to demonstrate the first multifunctional stretchable and self-healable electronic skin system (MSES) integrated with a strain monitor (top and left; red dashed box), an ECG sensor (bottom and left; magenta dashed box), and a LEC array (top and right; blue dashed box) using intrinsically stretchable materials (Figs. 5a and 5b and see Methods). A key constraint of previous wearable devices for highly integrated electronics is the challenge to efficiently integrate various components into a single onboard system (often due to different complex requirements for fabrication of each components). In this work, such an integrated system was achieved by the self-bonding process of each electronic module onto a PDMS-$MPU_{0.4}$-$IU_{0.6}$ substrate, which possesses exceptional mechanical properties such as high toughness, high stretchability, and self-healability even at room temperature (Supplementary Fig. 24). The fabrication process of each device begins with the AgNW network embedded in the surface of the self-healing polymer. To enable better electrical connection to the MSES platform, we applied flexible conductive cables to the electrical terminals. The self-healing polymer was also used to encapsulate the MSES system from external damages or moisture. Furthermore, to minimize bending-induced strains, the dielectric (strain sensor) and Cu-doped ZnS particle-incorporated emissive (LEC) layers were both placed on a neutral mechanical plane.

The MSES can thus now be conformably mounted onto human skin due to its low modulus and high stretchability (Fig. 5b and inset).

Figure 6a depicts an overview of the full system functionality where data from self-healable sensors were collected from the surface of the human body, subsequently processed and transmitted wirelessly to the self-healable LEC display for visual interpretation (Supplementary Fig. 25 and Methods). Figure 6b presents a 12s snippet from a 3-minute ECG data acquisition that was performed with the ECG electrodes. Each peak of the ECG signals was correctly detected (top). Based on our design, the heart-shaped LEC pixel blinks at each rise of the ECG signal as the R-peak of the waveform was approached (Fig. 6c). Figure 6d presents the heart rate changes that were successfully captured by our ECG electrodes. Figure 6e presents the output of the capacitive self-healable strain sensor as a function of strain. Figures 6d and 6e include colour band information (R1 to R5) regarding the mapping of the monitored signal regions to the LEC pixels. 5 of the pixel bars turned on or off in accordance to the heart rate or strain values based on the application and the corresponding threshold values, derived through wireless communication (Supplementary Figs. 26 and 27, see Supplementary Movie 4 and 5).

Conclusion

We showed the ability for conductive one-dimensional nanostructured network to reconstruct and to subsequently regain both conductivity and mechanical properties when in contact with dynamic supramolecular crosslinked polymer network. Compared to other self-healing electrodes, our utilised nanomaterial/polymer composite electrodes are highly

advantages due to their ability to be: (i) used as active components in devices (in addition to as interconnects), (ii) high stretchability even after damage, (iii) self-healing and high robustness, and (iv) autonomous self-healability at room temperature. With these attributes, we proceed to fabricate a fully-integrated electronic/optoelectronic multi-functional self-healable electronic system with human skin-like intrinsic stretchability and self-recoverability, which is simply based on a self-bonding assembly process. Within the self-healable onboard system, the high-performance interconnects, ECG/strain sensors, and LEC cells can now all seamlessly be integrated into a single platform by utilising the self-bonding property of the self-healing polymer, rendering it highly applicable for advanced robotic or prosthetic electronic skin. Furthermore, the recorded physiological data by each sensor can wirelessly be transmitted to the LEC array to provide continuous monitoring in real-time. Our described system-level multi-functionality self-healable electronic skin reinforces the future potential in realising future robust, and even unbreakable, electronics.

Methods

Preparation of CNT-based self-healable electrode

Single-walled carbon nanotubes purchased from Carbon Solutions Inc. (P2-SWNTs, 10 mg) were dispersed in chloroform solution (60 ml) using a tip horn sonicator. The dispersed CNT solution was spray-coated on the octadecyltrimethoxysilane (OTMS)-functionalised Si wafer using a commercial airbrush (Master Airbrush, Model SB844-SET)[8]. The CNT film thickness was measured by surface profiler (Bruker Dektak 150). As-prepared PDMS-$MPU_{0.4}$-IU_0 solution (0.15 g/ml in chloroform solvent) is poured onto the CNT film and then cured at room temperature for 12 h. The composite film can be easily detached from the handling substrate due to weak interaction between OTMS and the self-healing polymer.

Electrical measurement of self-healable stretchable electrode

To make a good contact to CNT or AgNW, we used Ag paste or conductive flexible cables such as anisotropic conductive film or thermally deposited Au/Cr on a poly(ethylene terephthalate) (PET) film. Electrical measurement of self-healable electrode was performed using a LCR meter (Agilent E4980A) while making a cut on or introducing a notch into the electrode. Furthermore, cyclic stretching-releasing tests were done on a linear stretcher controlled by a LabView software for automatic recording of stretching cycles.

Fabrication and electrical measurement of self-healable interconnects, ECG, and strain sensors

The schematic description of the fabrication process for each device is shown in Fig. 1a.. Initially AgNW (Zhejiang KECHUANG advanced materials technology co., ltd.) is dispersed in isopropanol (30 ml; diluted solution in 1:10). Then, AgNW solution is spray-coated onto the OTMS-functionalised SiO_2/Si wafer. Self-healing polymer solution (PDMS-$MPU_{0.4}$-$IU_{0.6\ of}$ ~3 g in ~20 ml $CHCl_3$, a 4-inch wafer size) is poured into the AgNW networked film on the sacrificial layer, which follows the same method of previous results[31]. After 12 h, at room temperature, we can peel off the self-healable electrode from the sacrificial wafer. For the interconnection, we used a shadow mask to define line-shaped AgNW film patterns, and then we followed the above the process. Furthermore, ECG sensor is made by mounting 2 electrodes on the top of the self-healing dielectric film and followed by attaching 1 electrode on the bottom of the film at r.t.. Finally, strain sensor fabrication process begins with the assembly of an insulating surface of 1 electrode onto the conducting side of the other electrode. The capacitive structure is mounted on the self-healing substrate and then encapsulated by the same layer without using heat or additives. Resistance or capacitance values of interconnect or strain sensor were measured using a LCR meter (Agilent E4980A) while making damages on or introducing a notch into each device. In addition to the electrical measurement, elastic recovery of a self-healable electrode in vertical direction was monitored by a force gauge (Series 5 Force Gauges, MARK-10 Corporation).

Fabrication of self-healable LEC

Cu-doped ZnS microparticles[36,37] mixed with our self-healing polymer with mass ratio of 1:1 were dispersed in

chloroform solution. The solution can be drop-casted or spin-coated on the OTMS-functionalised Si wafer and then cured for 6 h. The film thickness is about ~100 μm. The assembled emission layer was peeled off from the handling wafer and then transfer-printed on the bottom self-healable electrode. The top electrode was mounted onto the the other side of the emission layer. Such the assembly process was performed without external stimuli by virtue of its hydrogen bonding.

Fabrication of LEC array

The fabrication starts with as-prepared 2 self-healable electrodes (heart-shape and 5-bar pixels were created by using a shadow mask) and Cu-doped ZnS electroluminescent phosphor particles embedded in a self-healable polymer matrix. The emission layer is sandwiched between the electrodes for 3 h to make a reliable contact. Flexible conductive cables (Elform) were attached onto each electrode and then the LEC device was encapsulated with a self-healing film. The LEC device is transfer-printed onto the other self-healable substrate.

ECG/strain sensing and feedback display using wireless communication

The complete self-healable system (sensors & display) was also evaluated for a closed loop type application where ECG and strain data are real-time streamed from the measurement location to the self-healable LEC display to provide continuous feedback to the user. In this setup, the measurement system was coupled to a Bluetooth enabled Simblee (RFdigital) microcontroller (Simblee -1 / Transmitter Unit) that functioned in standalone mode with a 3.3V Li-ion battery as power source. In parallel, a second microcontroller (Simblee -2 / Receiver Unit) was programmed to control the self-healableLEC pixels based on the values it received wirelessly from Simblee -1. Simblee – 2 controlled the pixels by toggling the on-off state of a series of appropriately selected reed relays (Stadex-Meder SHV05-1A85-78L2K) while simultaneously streaming data to the previously described Java applet for data recording and visual confirmation of data quality. For the ECG sensor, the heart shaped pixel blinked at each ECG R-peak detection (based on an adapted Pan-Tompkins algorithm), while the bar pixels corresponded to HR regions ranging from < 60 to > 90 bpm with an interval of 10 bpm. For the strain sensor, the

capacitance output was measured with a capacitance to digital chip (Texas Instruments FDC 1004) and the bar pixels corresponded to strain regions ranging from 0% to 30% strain with 5% strain intervals.

Other materials and methods

More detailed information about other materials and methods is in supplementary information.

Data availability

The data sets generated during and/or analysed during current study are available from the corresponding authors upon reasonable request.

References

1. Kim, D.-H., *et al.* Epidermal electronics. *Science* **333**, 838-843 (2011).
2. Son, D., *et al.* Multifunctional wearable devices for diagnosis and therapy of movement disorders. *Nat. Nanotechnol.* **9**, 397-404 (2014).
3. Kaltenbrunner, M., *et al.* An ultra-lightweight design for imperceptible plastic electronics. *Nature* **499**, 458-463 (2013).
4. Gao, W., *et al.* Fully integrated wearable sensor arrays for multiplexed in situ perspiration analysis. *Nature* **529**, 509-514 (2016).
5. Yu, B., *et al.* An elastic second skin. *Nat. Mater.* **15**, 911-918 (2016).
6. Chortos, A., Liu, J. & Bao, Z. Pursuing prosthetic electronic skin. *Nat. Mater.* **15**, 937-950 (2016).
7. Kim, D.-H., *et al.* Materials for multifunctional balloon catheters with capabilities in cardiac electrophysiological mapping and ablation therapy. *Nat. Mater.* **10**, 316-323 (2011).
8. Oh, J. Y., *et al.* Intrinsically stretchable and healable semiconducting polymer for organic

transistors. *Nature* **539**, 411-415 (2016).

9. Ma, R., *et al.* Highly efficient electrocaloric cooling with electrostatic actuation. *Science* **357**, 1130-1134 (2017).

10. Liang, J., Li, L., Niu, X., Yu, Z. & Pei, Q. Elastomeric polymer light-emitting devices and displays. *Nat. Photonics* **7**, 817-824 (2013).

11. Matsuhisa, N., *et al.* Printable elastic conductors by in situ formation of silver nanoparticles from silver flakes. *Nat. Mater.* **16**, 834-840 (2017).

12. Park, M., *et al.* Highly stretchable electric circuits from a composite material of silver nanoparticles and elastomeric fibres. *Nat. Nanotechnol.* **7**, 803-809 (2012).

13. Sun, J.-Y., *et al.* Highly stretchable and tough hydrogels. *Nature* **489**, 133-136 (2016).

14. Yuk, H., Zhang, T., Parada, G. A., Liu, X. & Zhao, X. Skin-inspired hydrogel–elastomer hybrids with robust interfaces and functional microstructures. *Nat. Commun*. **7**:12028 doi: 10.1038/ncomms12028 (2016).

15. Savagatrup, S., *et al.* Plasticization of PEDOT:PSS by Common Additives for Mechanically Robust Organic Solar Cells and Wearable Sensors. *Adv. Funct. Mater.* **25,** 427-436 (2015).

16. Zhao, H., O'brien, K., Li, S. & Shepherd, R. F. Optoelectronically innervated soft prosthetic hand via stretchable optical waveguides. *Sci. Robot.* **1**, eaai7529 (2016).

17. Xu, J., *et al.* Highly stretchable polymer semiconductor films through the nanoconfinement effect. *Science* **355**, 59-64 (2017).

18. Yang, Y. & Urban, M. W. Self-healing polymeric materials. *Chem. Soc. Rev.* **42**, 7446-7467 (2013).

19. Holten-Andersen, N., *et al.* pH-induced metal-ligand cross-links inspired by mussel yield self-healing polymer networks with near-covalent elastic moduli. *Proc. Natl. Acad. Sci.* **108**, 2651-2655 (2011).

20. Yuan, L., *et al.* Poly(phenylene oxide) modified cyanate resin for self-healing. *Polym. Adv. Technol.* **25**, 752-759 (2014).

21. Li, C.-H., *et al*. A highly stretchable autonomous self-healing elastomer. *Nature Chem.* **8**, 618-624 (2016).

22. Huang, Y., *et al*. A self-healable and highly stretchable supercapacitor based on a dual crosslinked polyelectrolyte. *Nat. Commun*. **6**:10310 doi: 10.1038/ncomms10310 (2015).

23. Gong, C., *et al.* A healable, semitransparent silver nanowire-polymer composite conductor. *Adv. Mater.* **25**, 4186-4191 (2013).

24. Li, J., *et al.* Healable capacitive touch screen sensors based on transparent composite electrodes comprising silver nanowires and a Furan/Maleimide Diels-Alder cycloaddition polymer. *ACS Nano* **8**, 12874-12882 (2014).

25. Wang, H., *et al.,* A Mechanically and Electrically Self-Healing Supercapacitor. *Adv. Mater.* **26**, 3638-3643 (2014).

26. Bandodkar, A. J., *et al.* All-printed magnetically self-healing electrochemical devices. *Sci. Adv.* **2**:e1601465 (2016).

27. Huynh, T.-P. & Haick, H. Self-healing, fully functional, and multiparametric flexible sensing platform. *Adv. Mater.* **28**, 138-143 (2016).

28. Cordier, P., Tournilhac, F., Soulie-Ziakovic, C. & Leibler, L. Self-healing and thermoreversible rubber from supramolecular assembly. *Nature* **451**, 977-980 (2008).

29. Zou, Z., *et al.* Rehealable, fully recyclable, and malleable electronic skin enabled by dynamic covalent thermoset nanocomposite. *Sci. Adv.* **4**: 2, eaaq0508 (2018).

30. Palleau, E., *et al.* Self-healing stretchable wires for reconfigurable circuit wiring and 3D microfluidics. *Adv. Mater.* **25**, 1589-1592 (2013).

31. Kang, J., *et al.* Tough and water-insensitive self-healing elastomer for robust electronic skin. *Adv. Mater.* **30***,* 1706846 (2018).

32. De Greef, T. F. A., *et al*. Supramolecular polymerization. *Chem. Rev.* **109**, 5687–5754 (2009).

33. Kim, S. M., *et al*. Role of anions in the $AuCl_3$-doping of carbon nanotubes. *ACS Nano* **5**, 1236-1242 (2011).

34. Lipomi, D. J., *et al.* Skin-like pressure and strain sensors based on transparent elastic films of carbon nanotubes. *Nature Nanotechnol.* **6**, 788-792 (2011).

35. Wallace, W. E., *et al.* Polymer chain relaxation: surface outpaces bulk. *Macromolecules* **34**, 5081-5082 (2001).

448 36. Larson, C., *et al*., Highly stretchable electroluminescent skin for optical signaling and
449 tactile sensing. *Science* **351**, 1071-1074 (2016).

450 37. Yang, C. H., *et al*., Electroluminescence of giant stretchability. *Adv. Mater.* **28**, 4480-4484
451 (2016).

452

Acknowledgements

This work is supported by Samsung Electronics. O.V. was supported by the Swiss National Science Foundation "Mobility Fellowship" P2ELP2_165147.

Author Contributions

D.S., J.K., O.V., and Z.B. designed the experiments. D.S., J.K., O.V., N.M., Y.K., J.Y.O., J.W.T., J.M., M.K., T.K., Y.L., A.F.M., M.K., F.M.L., J.H., U.K., Y.L., Y.Y., J.B.-H.T. Z.B. performed experiments and analysis. D.S., J.K., O.V., J.B.-H.T., and Z.B. wrote the paper.

Competing Financial Interests

The authors declare no competing financial interest.

Additional Information

Supplementary information is available in the online version of the paper. Reprints and permissions information is available online at www.nature.com/reprints. Correspondence and requests for materials should be addressed to Z.B..

Figure Legends

Figure 1 | Schematic drawings of dynamic reconstruction of conductive nano-network in the tough and stretchable self-healing polymer matrix. a, Schematic illustration of the fabrication process of self-healable stretchable electrode by embedding a carbon nanotube (CNT) conductive network into the self-healing polymer matrix. **b,** Sequential schematic illustration of different types of substrates and their response to damage and reconstruction. Making a cut on the surface of CNT/ polymer composite electrode is defined as "mechanical damage". Non-healable elastomers cannot sustain strain after mechanical damage (top, orange-coloured schematic). Viscoelastic polymer may be mechanically stretched after reconnecting and heating, but the conducting network cannot reconstruct and will hence lose conductivity upon stretching (middle, pink-coloured schematic). Tough self-healing elastomer results in electrodes with both high mechanical and electrical performance even after mechanical damage, owing to its self-recoverability and high toughness (bottom, blue/green-coloured schematic in a red box). **c,** Proposed recovery mechanism for carbon nanotubes embedded in self-healing polymer matrix. The CNT network reconstruction is based on observations as follows: (1) continuous reduction of resistance over time, (2) recovery of stretchability, (3) maintaining high conductivity with strain for recovered electrode, (4) lack of clear physical separation in the CNT network in the recovered cut region. The electrode was autonomously electrically healed owing to the dynamic nature of the self-healing polymer, allowing CNT network to rearrange and recover both stretchability and conductivity. The numbers in the plot of resistance of the self-healable electrode as a function of time correspond to the numbered schematics.

Figure 2 | Dynamic reconstruction of one-dimensional conductive nano-network. a, Plot

(bottom) indicates electrical characteristics of self-healable CNT/PDMS-$MPU_{0.4}$-$IU_{0.6}$ composite electrode as a function of time while making damages with different mechanical strength (0.5 N and 4 N). In addition, top plot shows the self-healing performance of the CNT/PDMS-$MPU_{0.4}$-$IU_{0.6}$ composite electrode after 4 N cutting and even 20 times of 2 N cuttings. **b,** OM images of self-healable CNT/PDMS-$MPU_{0.4}$-$IU_{0.6}$ composite electrodes be fore and after self-healing (12 h). The self-healed CNT network was robust even after stretching up to 100% strain (bottom images. **c,** Plot of resistance of self-healable CNT/PDMS-$MPU_{0.4}$-$IU_{0.6}$ composite electrode as a function of strain with different self-healing periods of time after 2N cutting. **d,** Plots of resistance of pristine (red) and self-healed (blue) CNT/PDMS-$MPU_{0.4}$-$IU_{0.6}$ composite electrodes as a function of strain after making a cut and self-healing for 12 h. **e,** Real-time electrical monitoring of reconstruction of CNT/PDMS-$MPU_{0.4}$-$IU_{0.6}$ (top, red) and AgNW/PDMS-$MPU_{0.4}$-$IU_{0.6}$ (bottom, blue) after cutting and reconnection. **f,** SEM images of self-healable CNT/PDMS-$MPU_{0.4}$-$IU_{0.6}$ (top, red) and AgNW/PDMS-$MPU_{0.4}$-$IU_{0.6}$ (bottom, blue) composite electrodes before and after self-healing (12 h). **g,** Normalized resistance change of 3 kinds of composite electrodes (red, CNT/PDMS-$MPU_{0.4}$-$IU_{0.6}$; green, CNT/SEBS; blue, CNT/PDMS) as a function time is measured while making a cut on the surface of each electrode and **h,** after stretching them up to 100% tensile strain and 2 days. We used a force gauge to control the force used for cutting.

Figure 3 | Interconnection and sensors with autonomous Self-healability. a, Plot of relative resistance change of AgNW with 3 different thicknesses as functions of strain (red, AgNW 114 nm; blue, 317 nm; green, 702 nm). Inset shows a photograph of each electrode. **b,** Top frame shows a plot of resistance of damage-resistant electrode with different AgNW thickness as a

function of time while making consecutive 3 cuts (2 N each) (top). Bottom shows magnified low-resistance range. **c,** Images (top 2 frames) of sequential self-recovery process of self-healable AgNW/PDMS-$MPU_{0.4}$-$IU_{0.6}$ composite electrode even under an artificial sweat solution. After the autonomous healing process, the healed electrode is stretched up to 50% strain (bottom 2 frames). **d,** Photographs (top and left, partial cut; top and right, complete cut; bottom, self-healed) of the self-healable interconnects interfaced with commercial LEDs and passive modules on polyimide substrates. Autonomously healed 1st interconnect is stretched well to deliver electrical power to 2nd LED cell (bottom). **e,** Image and corresponding schematic of self-healable ECG sensor. **f,** Cardiac signals measured from the self-healable ECG sensor (red) and commercial one (black) are shown for comparison. Blue highlighted section shows the electrode pads were damaged and subsequently recovered in a few seconds. **g,** Strain sensitivity comparison and **h,** stretching cyclic (30% strain) test between before (red) and after (blue) making a partial cut on the strain sensor. Inset shows the damaged strain sensor. **i,** The strain sensor with a notch (insets) still shows good stretchability without any electrical loss owing to the high toughness of the polymer substrate that is capable of minimizing crack propagations.

Figure 4 | Highly stretchable electroluminescent skin with autonomous self-healability. a, **a,** Strain sensing capability of pristine and self-healable LEC devices. Inset images show the bisected and autonomous healed capacitive LEC devices. **b,** LEC with notch is stretched

without breaking. Images show that no crack propagation in presence of the notch proceeded owing to high fracture toughness of the self-healing polymer matrix. **c,** We applied 200 V and 250 Hz of AC electric field to the CNT-based LEC. In the meantime, we stretched it up to 250% tensile strain to confirm its high stretchability. **d,** Photographs of cut and self-healed (after a day) self-healable CNT-based LEC device. After a day, **e,** the self-healed CNT and **f,** AgNW LEC devices still show reliable stretchability while giving a stable light. **g,** Image of LEC encapsulated with self-healing polymer layers. It shows an image of AgNW LEC after dipping/pulling cycles under water. **h,** Images of pristine and **i,** stretched LEC device under water.

Figure 5 | Schematic drawings and corresponding images of an integrated self-healable electronic skin system. a, Schematic multifunctional self-healable electronic skin system consists of strain sensor with a capacitive structure (top center and left insets show its layer information; red arrows indicate that each electrode is assembled on the desired surfaces), ECG sensor (bottom center and left insets show its assembly process), and LEC array (right and bottom insets indicate its fabrication owing to hydrogen bonding-driven facile assembly). **b,** Multifunctional self-healable electronic skin device on skin while performing the LEC operation which emits a blue-green light. Inset shows the e-skin on the rigid substrate.

Figure 6 | Demonstration of the integrated self-healable electronic skin system. a,

Overview of the system with sensors communicating wirelessly values to the display. **b,** ECG waveforms sampled at 500 Hz measured by the self-healing device. **c,** self-healable LEC heart shaped pixel that blinks when a heart beat is detected. **d,** Heart rate is monitored by self-healable ECG sensor. **e,** Response of the strain sensor to a 30% stretch load and unload. **f,** Self-healable LEC bar pixels turning on and off based on the value of heart rate.

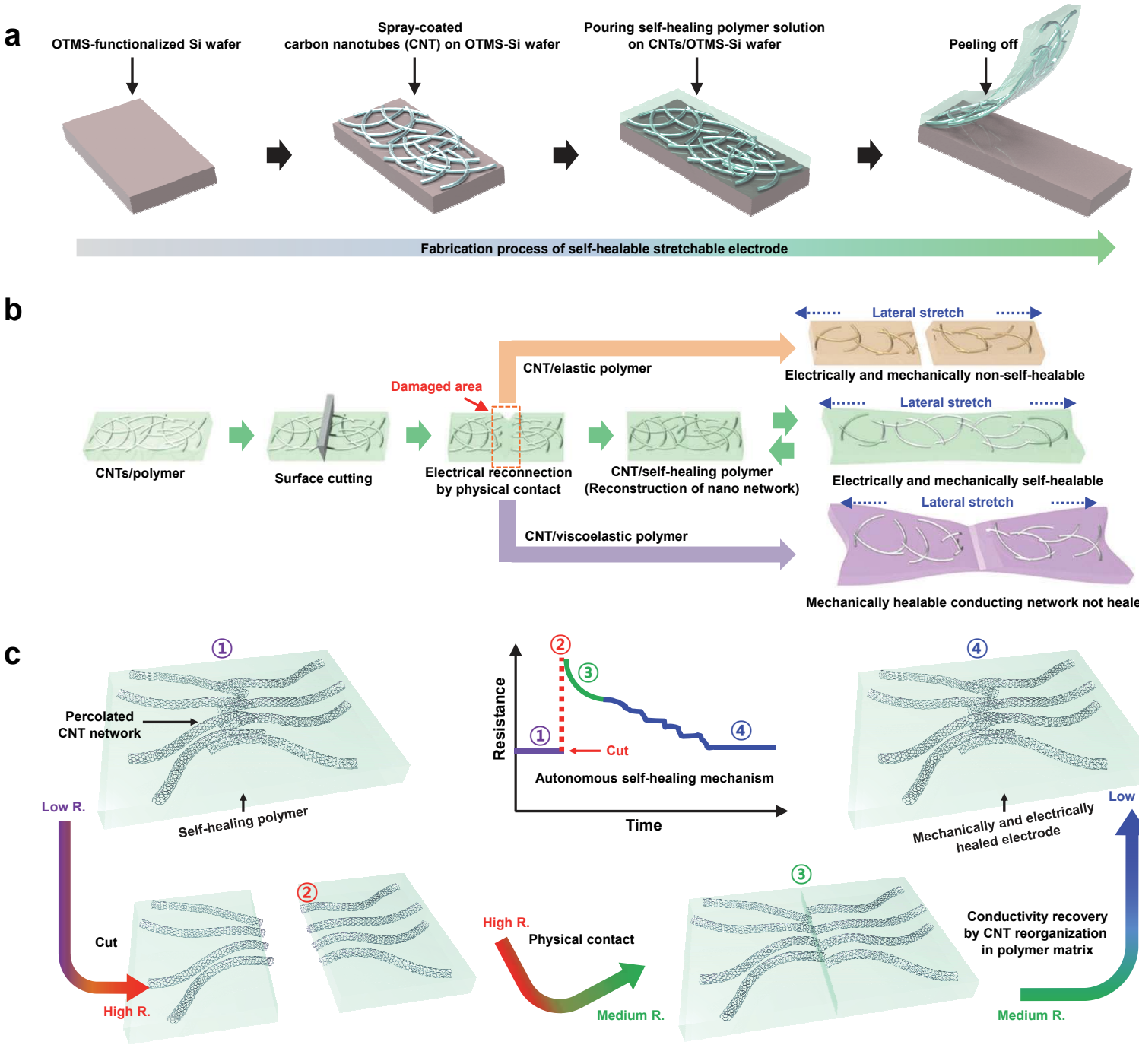
a
OTMS-functionalized Si wafer
Spray-coated
carbon nanotubes (CNT) on OTMS-Si wafer
Pouring self-healing polymer solution
on CNTs/OTMS-Si wafer
Peeling off
Fabrication process of self-healable stretchable electrode
b
CNTs/polymer
Surface cutting
Damaged area
Electrical reconnection
by physical contact
CNT/self-healing polymer
(Reconstruction of nano network)
CNT/elastic polymer
CNT/viscoelastic polymer
Lateral stretch
Electrically and mechanically non-self-healable
Lateral stretch
Electrically and mechanically self-healable
Lateral stretch
Mechanically healable conducting network not healed
c
Percolated
CNT network
Self-healing polymer
Low R.
Cut
High R.
Resistance
Time
Cut
Autonomous self-healing mechanism
High R.
Physical contact
Medium R.
Mechanically and electrically
healed electrode
Low R.
Conductivity recovery
by CNT reorganization
in polymer matrix
Medium R.

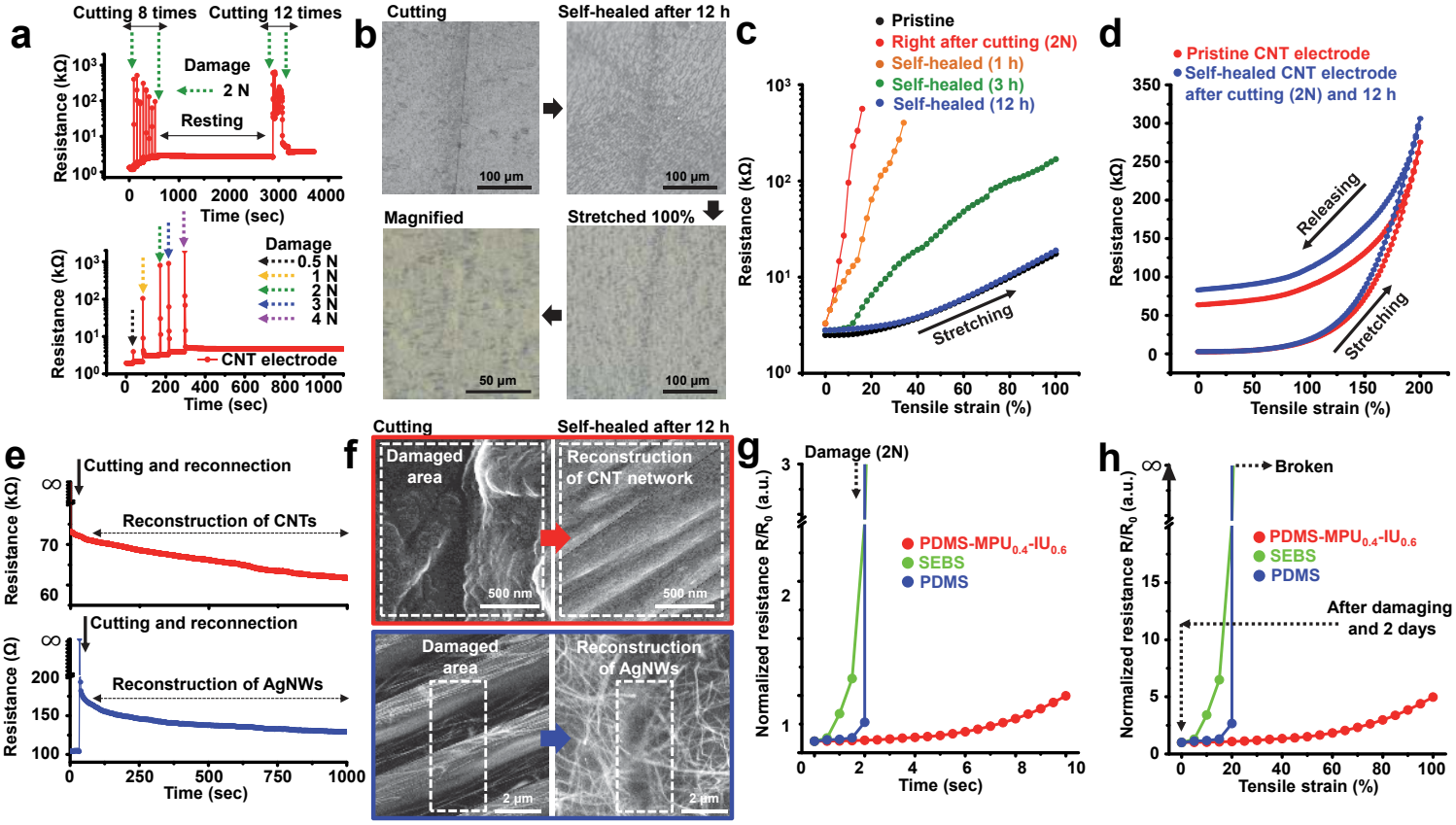
a
Cutting 8 times
Cutting 12 times
Damage
2 N
Resting
Resistance (kΩ)
Time (sec)
Damage
0.5 N
1 N
2 N
3 N
4 N
CNT electrode
b
Cutting
Self-healed after 12 h
Magnified
Stretched 100%
100 μm
50 μm
c
Pristine
Right after cutting (2N)
Self-healed (1 h)
Self-healed (3 h)
Self-healed (12 h)
Stretching
Tensile strain (%)
d
Pristine CNT electrode
Self-healed CNT electrode
after cutting (2N) and 12 h
Releasing
Stretching
e
Cutting and reconnection
Reconstruction of CNTs
Reconstruction of AgNWs
f
Damaged area
Reconstruction of CNT network
Reconstruction of AgNWs
500 nm
2 μm
g
Damage (2N)
PDMS-MPU0.4-IU0.6
SEBS
PDMS
Normalized resistance R/R0 (a.u.)
h
Broken
After damaging and 2 days

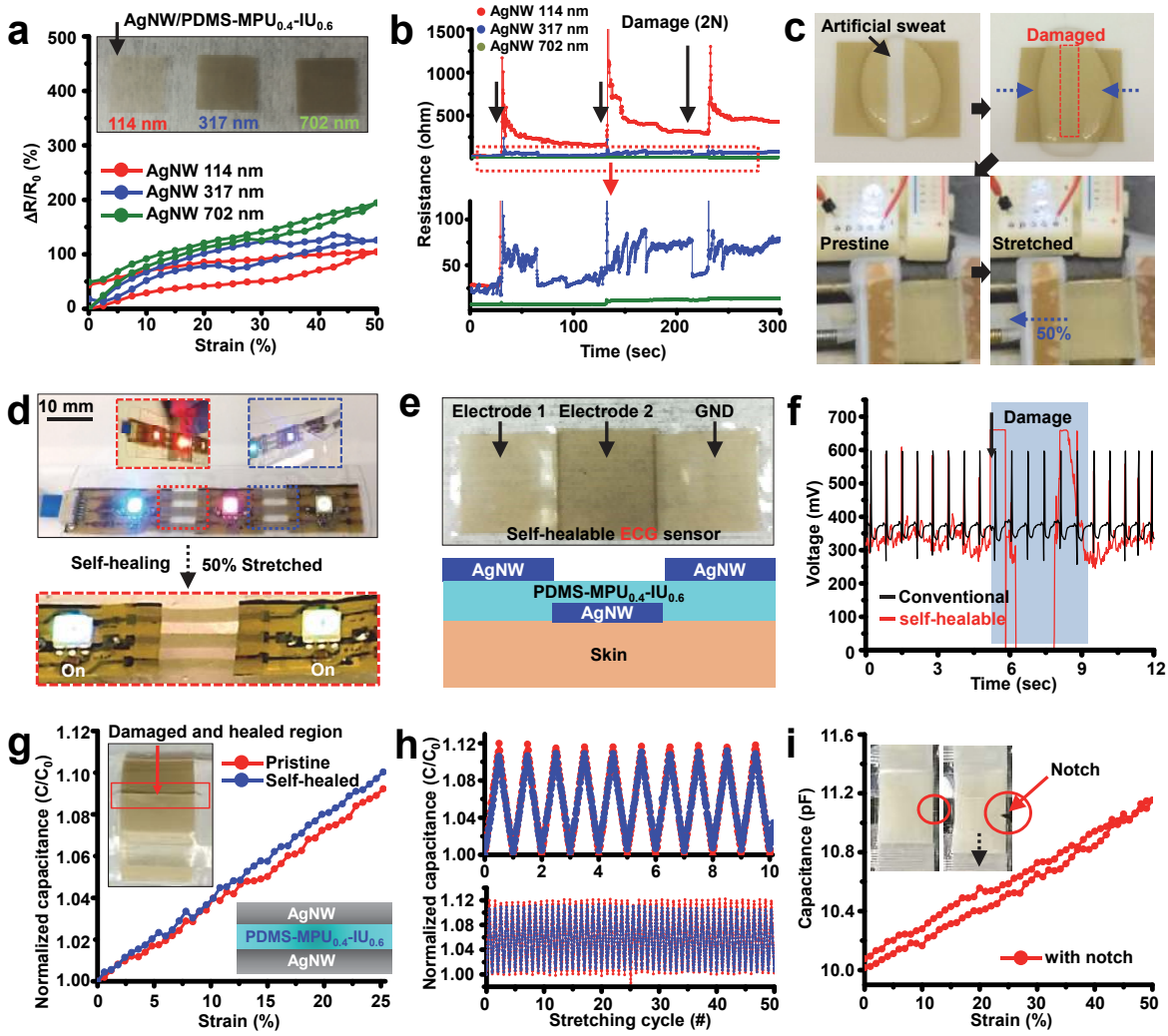
a
AgNW/PDMS-MPU0.4-IU0.6
114 nm
317 nm
702 nm
ΔR/R0 (%)
AgNW 114 nm
AgNW 317 nm
AgNW 702 nm
Strain (%)
b
AgNW 114 nm
AgNW 317 nm
AgNW 702 nm
Damage (2N)
Resistance (ohm)
Time (sec)
c
Artificial sweat
Damaged
Prestine
Stretched
50%
d
10 mm
Self-healing
50% Stretched
On
On
e
Electrode 1
Electrode 2
GND
Self-healable ECG sensor
AgNW
AgNW
PDMS-MPU0.4-IU0.6
AgNW
Skin
f
Damage
Voltage (mV)
Conventional
self-healable
Time (sec)
g
Damaged and healed region
Pristine
Self-healed
AgNW
PDMS-MPU0.4-IU0.6
AgNW
Normalized capacitance (C/C0)
Strain (%)
h
Normalized capacitance (C/C0)
Stretching cycle (#)
i
Notch
Capacitance (pF)
with notch
Strain (%)

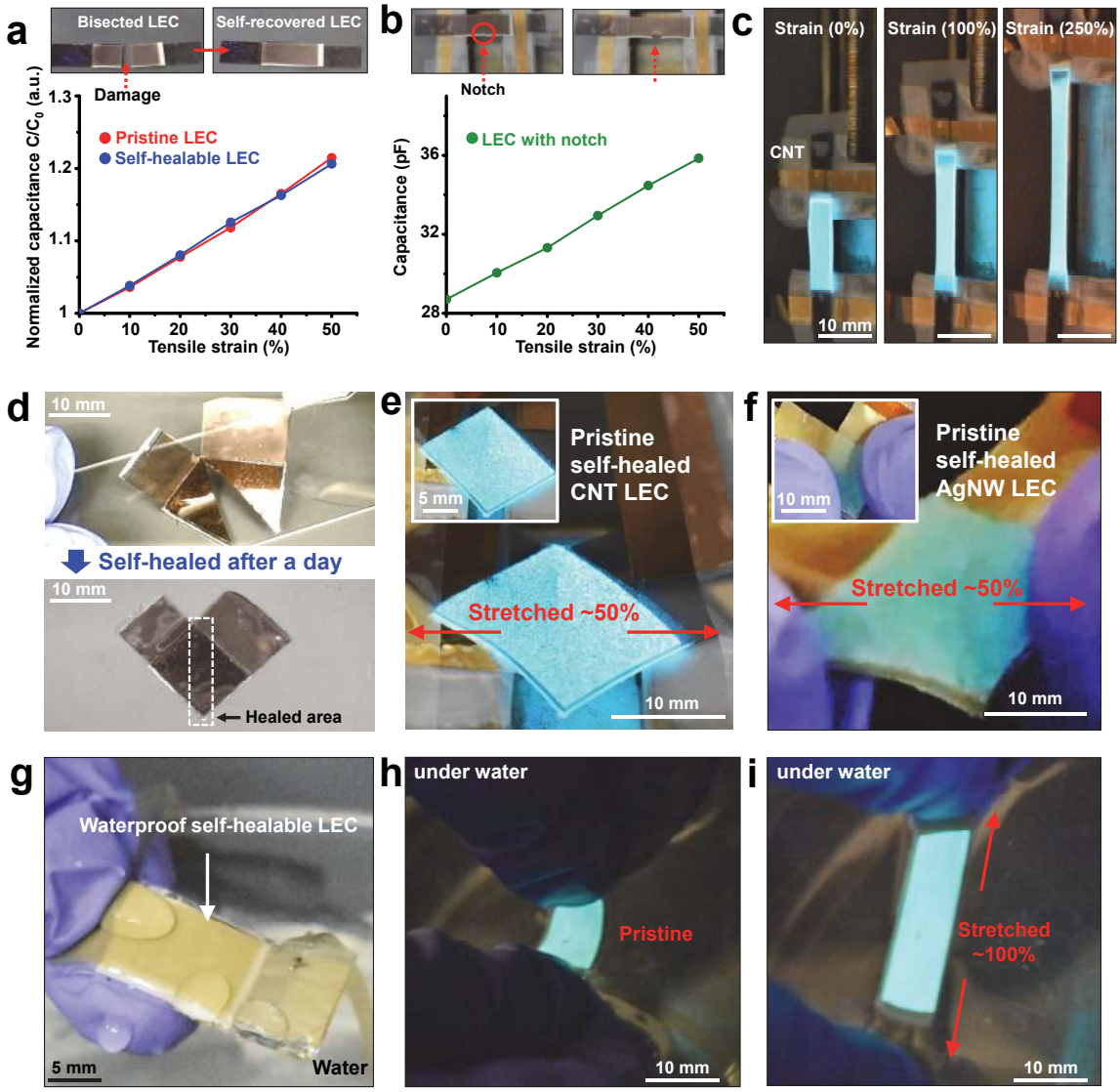
a
Bisected LEC
Self-recovered LEC
Damage
Pristine LEC
Self-healable LEC
Normalized capacitance C/C0 (a.u.)
Tensile strain (%)
b
Notch
LEC with notch
Capacitance (pF)
Tensile strain (%)
c
Strain (0%)
Strain (100%)
Strain (250%)
CNT
10 mm
d
10 mm
Self-healed after a day
Healed area
e
Pristine self-healed CNT LEC
5 mm
Stretched ~50%
10 mm
f
Pristine self-healed AgNW LEC
10 mm
Stretched ~50%
10 mm
g
Waterproof self-healable LEC
5 mm
Water
h
under water
Pristine
10 mm
i
under water
Stretched ~100%
10 mm

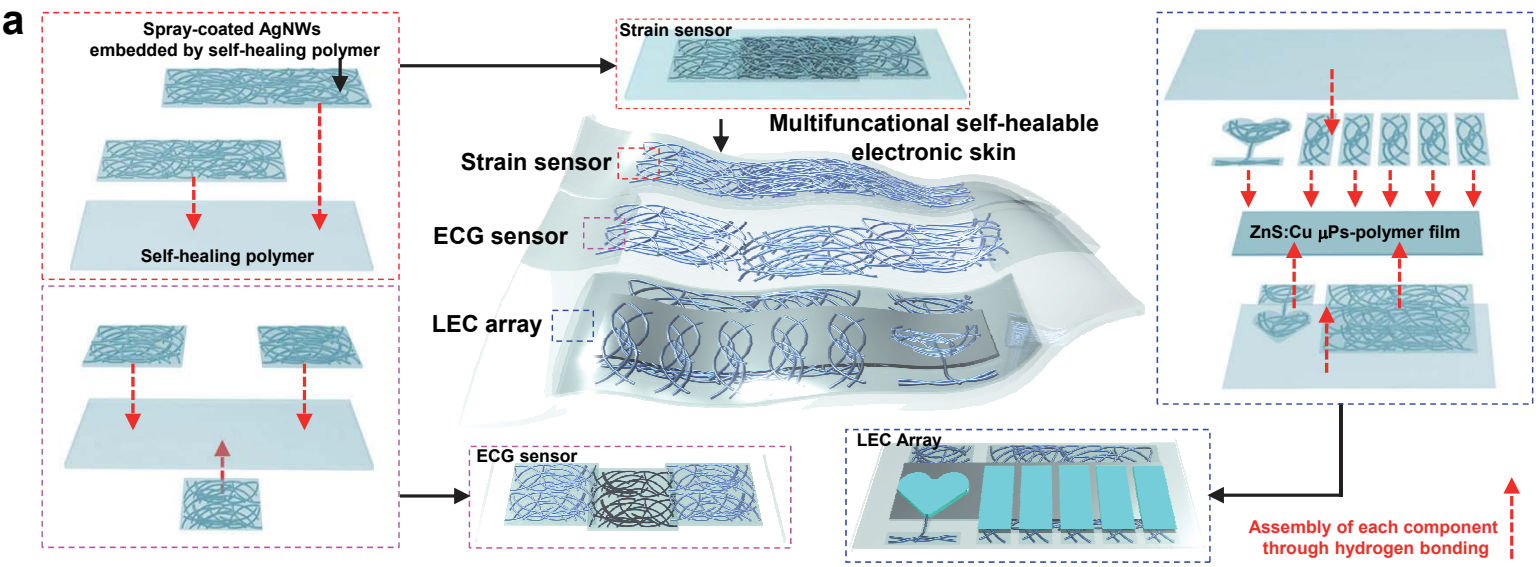
a
Spray-coated AgNWs
embedded by self-healing polymer
Self-healing polymer
Strain sensor
Multifuncational self-healable
electronic skin
Strain sensor
ECG sensor
LEC array
ZnS:Cu μPs-polymer film
ECG sensor
LEC Array
Assembly of each component
through hydrogen bonding

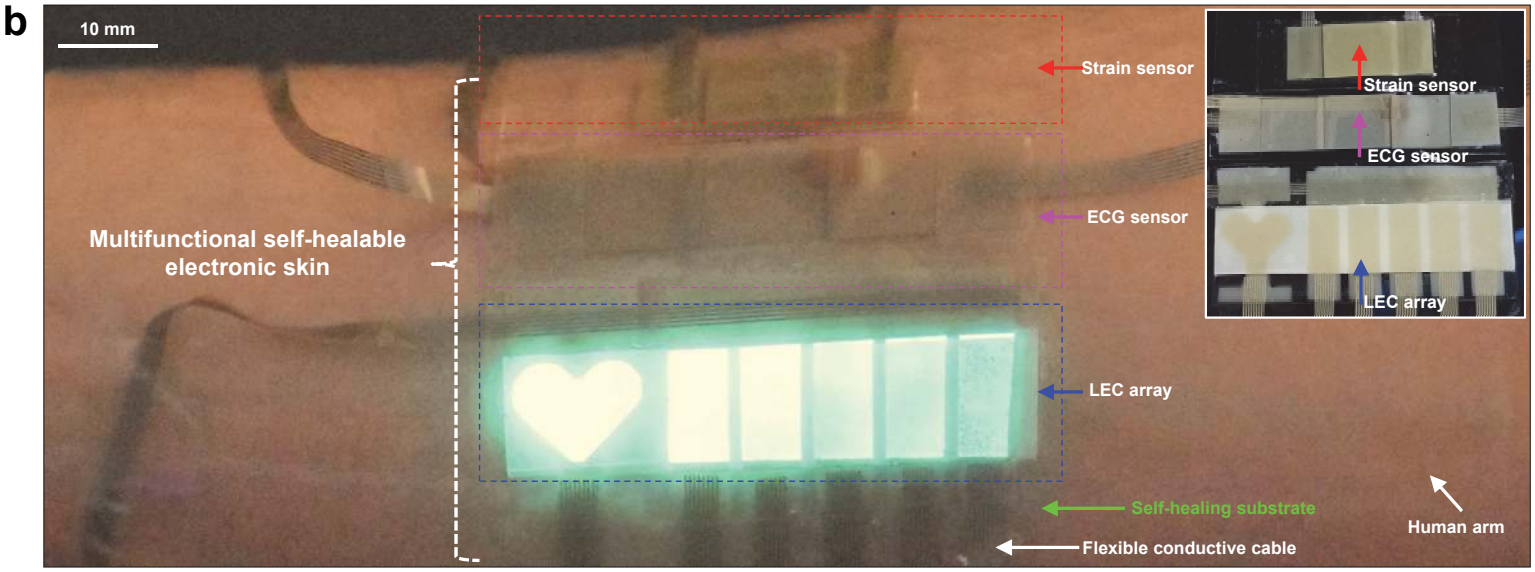
b
10 mm
Multifunctional self-healable
electronic skin
Strain sensor
ECG sensor
LEC array
Self-healing substrate
Flexible conductive cable
Human arm
Strain sensor
ECG sensor
LEC array

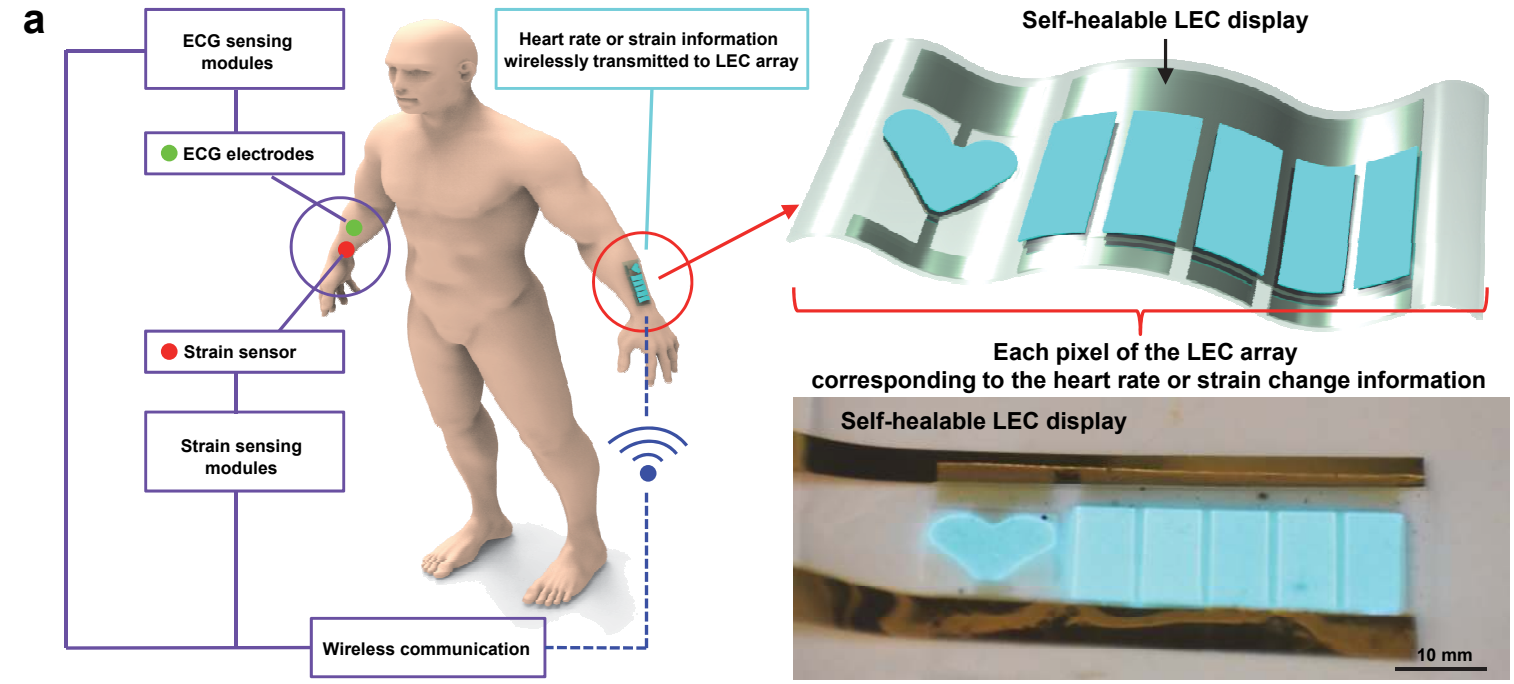
a
ECG sensing modules
ECG electrodes
Strain sensor
Strain sensing modules
Wireless communication
Heart rate or strain information wirelessly transmitted to LEC array
Self-healable LEC display
Each pixel of the LEC array corresponding to the heart rate or strain change information
Self-healable LEC display
10 mm

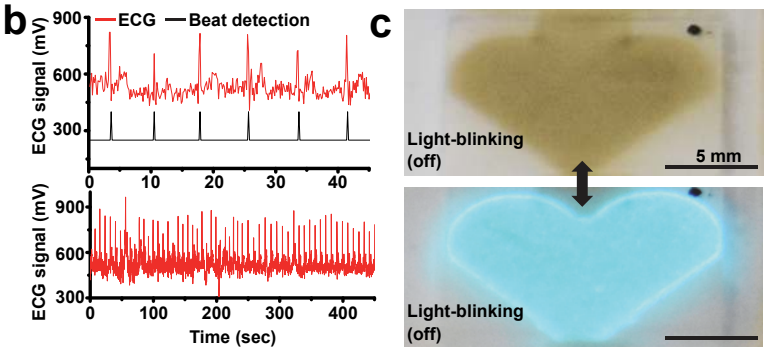
b
ECG
Beat detection
ECG signal (mV)
Time (sec)

c
Light-blinking (off)
5 mm
Light-blinking (off)

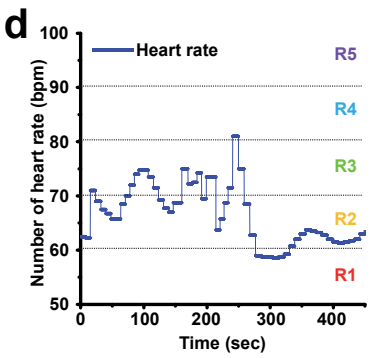
d
Heart rate
R5
R4
R3
R2
R1
Number of heart rate (bpm)
Time (sec)

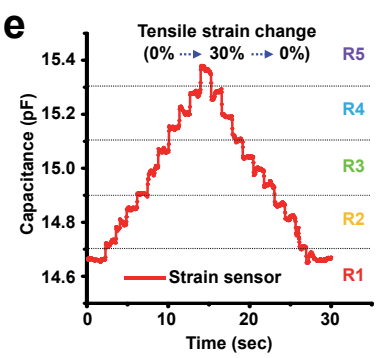
e
Tensile strain change
(0% 30% 0%)
R5
R4
R3
R2
R1
Capacitance (pF)
Strain sensor
Time (sec)

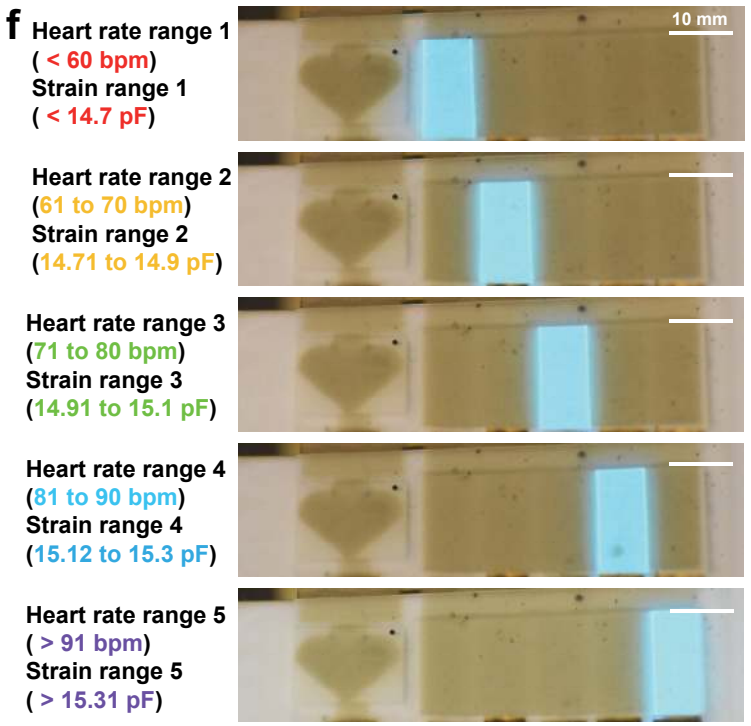
f
Heart rate range 1
(< 60 bpm)
Strain range 1
(< 14.7 pF)
Heart rate range 2
(61 to 70 bpm)
Strain range 2
(14.71 to 14.9 pF)
Heart rate range 3
(71 to 80 bpm)
Strain range 3
(14.91 to 15.1 pF)
Heart rate range 4
(81 to 90 bpm)
Strain range 4
(15.12 to 15.3 pF)
Heart rate range 5
(> 91 bpm)
Strain range 5
(> 15.31 pF)
10 mm